Performance Analysis of Carrier-Phase DGPS Navigation for Shipboard Landing of Aircraft

BORIS PERVAN and FANG-CHENG CHAN
Illinois Institute of Technology, Chicago, Illinois

DEMOZ GEBRE-EGZIABHER, SAM PULLEN, and PER ENGE
Stanford University, Stanford, California

GLENN COLBY
Naval Air Warfare Center, Patuxent River, Maryland

Received October 2002; Revised July 2003

ABSTRACT: *Shipboard-relative GPS (SRGPS) is a variant of the Joint Precision Approach and Landing System (JPALS) that is being developed to support automatic shipboard landings in zero-visibility conditions. At present, the navigation system requirements specify a vertical protection level of 1.1 m, an integrity risk of approximately 10^{-7}, and a system availability of at least 99.7 percent. Because of the stringent nature of these specifications, differential carrier-phase solutions are being pursued. In this context, this paper gives a detailed analysis of the fault-free integrity and availability of SRGPS. The performance of single- and dual-frequency architectures is evaluated for both floating-ambiguity and fixed-integer carrier-phase differential GPS (DGPS) navigation. The sensitivity of SRGPS availability is quantified with respect to raw code and carrier measurement quality, spatial decorrelation of ionospheric and tropospheric errors, and broadcast service radius. Necessary conditions to achieve the desired navigation performance are defined.*

INTRODUCTION

Shipboard-relative GPS (SRGPS) is an architectural variant of the Joint Precision Approach and Landing System (JPALS), which is being developed to provide high-accuracy and high-integrity differential GPS (DGPS) navigation for automatic shipboard landings. The required navigation system vertical accuracy is currently envisioned to be on the order of 0.3 m, and the vertical protection level is 1.1 m, with an associated integrity risk of approximately 10^{-7} [1]. To provide such navigation performance with adequate system availability—at least 99.7 percent [2]—differential carrier-phase solutions are presently being pursued [3].

The full availability of both the L1 and L2 GPS signals for this military application is tempered by the simultaneous need to provide redundancy in the event of hostile jamming or interference. In this respect, although dual-frequency architectures may be acceptable for SRGPS, single-frequency carrier-phase solutions (if possible) would be advantageous. In addition, controlled reception pattern (phased-array) shipboard antennas will be implemented in SRGPS to provide superior performance in a jamming environment and to mitigate multipath. These antennas can also be expected to benefit SRGPS performance by providing exceptionally precise code and carrier measurements at the reference station for satellites at all elevations [4].

The use of differential carrier phase for precise navigation is contingent upon the successful estimation or resolution of cycle ambiguities. While it is understood that fixed-integer implementations will provide better accuracy than floating-ambiguity implementations, the integrity of the cycle resolution process must be ensured. In the most general sense, cycle resolution integrity will be a function of the quality of the raw code and carrier measurements, satellite geometry, and filter duration. For example, a large service volume can potentially provide sufficient time for averaging of noisy measurements, and also for satellite motion, to improve cycle ambiguity observability. In this case, however, the spatial decorrelation of carrier-phase measurement errors (over the resulting long baselines) must be carefully accounted for.

It is intuitively clear that the performance of carrier-phase–based DGPS (for both floating-ambiguity

NAVIGATION: *Journal of The Institute of Navigation*
Vol. 50, No. 3, Fall 2003
Printed in the U.S.A.

and fixed-integer implementations) will be optimum if:

- Dual-frequency measurements are used (instead of L1 or L2 alone).
- The GPS data broadcast radius is large (ensuring longer filtering times and more satellite motion).
- High-performance receivers and antennas are used (to provide small raw code and carrier measurement error).

While these observations are all qualitatively true, in this work we seek *quantitative* design guidelines and trade-offs applicable to SRGPS. The following are some specific questions that require quantitative answers:

- Given a specified GPS data broadcast radius (or maximum filter duration), how small must raw measurement errors be to ensure adequate SRGPS availability? The answer to this question may be interpreted as a derived system requirement on antenna/receiver performance.
- Can we quantify the benefit to navigation availability due to fixing integers (relative to a floating implementation), given that the probability of incorrect integer fix must be consistent with integrity requirements? To what extent does integer fixing allow for the relaxation of requirements on antenna/receiver quality and/or GPS data broadcast radius?
- How sensitive is SRGPS performance to time-correlated multipath, residual tropospheric error decorrelation, and ionospheric spatial gradients?
- How do the answers to the above questions differ for single- and dual-frequency architectures?

In this paper, we seek to answer these questions to provide a basis for defining necessary conditions (i.e., derived requirements) to ensure adequate fault-free availability of SRGPS navigation. The development of fault detection methodologies for SRGPS is the subject of related concurrent work [5].

ANALYSIS METHODOLOGY

To explore the sensitivity of SRGPS performance to variations in system and measurement error characteristics, we used a covariance analysis methodology. A nominal fixed-wing (airplane) approach model, illustrated in Figure 1, was assumed in this analysis [6, 7].

The GPS data broadcast radius, also indicated in the figure, was treated as a parameter. Within the broadcast radius, code and carrier measurements from the shipboard reference receiver(s) were assumed to be available for use at the aircraft. In this analysis, filtering of aircraft and shipboard measurements was initiated at broadcast radius entry. (The implications of filtering prior to broadcast radius entry, which can be particularly advantageous for dual-frequency architectures, will be addressed later.) The nominal DO-229C (Wide Area Augmentation System [WAAS] Minimum Operational Performance Standards [MOPS]) [8] GPS satellite constellation, a Central Pacific ship location (22° N, 158° W), and a satellite elevation mask of 7.5 deg were used in the analysis. This satellite mask angle was selected as a representative value to account for potential obstructions in the shipboard environment, as well as loss of low-elevation lines of sight at the aircraft due to attitude motion. Both single- and dual-frequency implementations were considered in this work. The measurement error

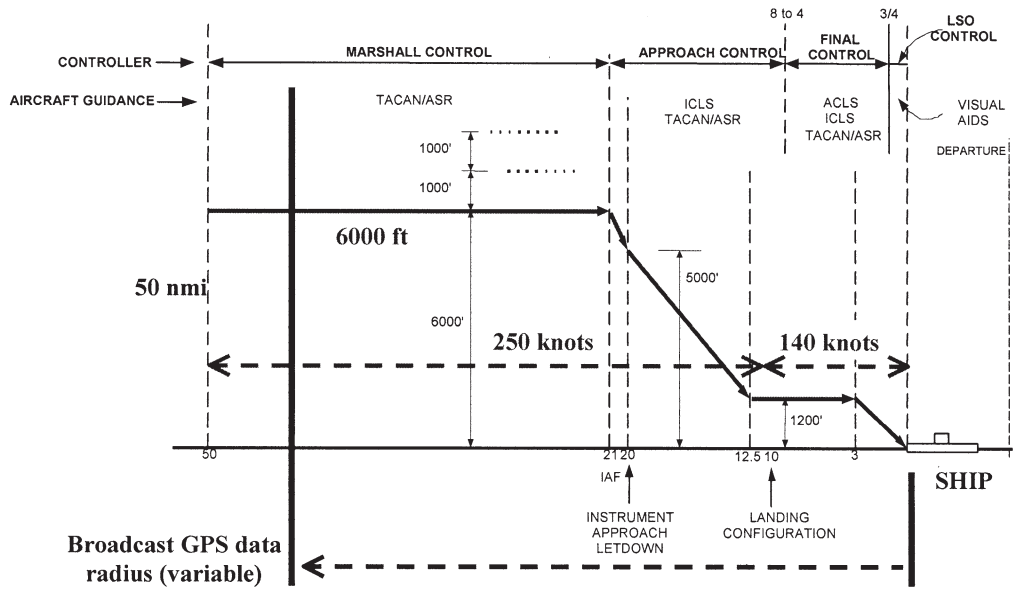

Fig. 1–Nominal Airplane Approach Model

models used in the covariance analysis, as well as details regarding the floating-ambiguity and fixed-integer implementations, are described below.

Multipath/Receiver Noise Error Model

Both code and carrier errors were modeled as first-order Gauss-Markov random processes (GMRPs). Independent GMRPs were assumed for code and carrier for each frequency and for each satellite. The associated GMRP standard deviations and time constants were treated as parameters that were varied in the analysis to quantify the effect of receiver/antenna quality on overall SRGPS performance. The time constants and standard deviations (for single-difference measurement error) used in this work were as follows:

- Time constant: $\tau \in \{40, 60, 120\}$ s
- P(Y)-code: $\sigma_{PR} \in \{0.1, 0.15, 0.3\}$ m
- Carrier: $\sigma_{\phi} \in \{0.5, 1.0, 1.5, 2.0\}$ cm

Each error standard deviation listed was applied to both L1 and L2 measurements for all satellites, independently of elevation. Each error time constant was applied to all measurement models.

Residual Tropospheric Decorrelation

Residual differential tropospheric error (i.e., the ranging error remaining after tropospheric correction) was modeled using the Local Area Augmentation System (LAAS) tropospheric error model [9]:

$$\varepsilon_{T}(i, k) = \Delta n \cdot \frac{h_0[1 - \exp(-h(k)/h_0)]}{\sqrt{0.002 + \sin^2 E(i, k)}} \quad (1)$$

where ε_T is the tropospheric error; Δn is the error in knowledge of local index of refraction; h_0 is the troposphere scale height; h is the altitude of the airplane; E is satellite elevation; and i and k are satellite and time indices, respectively.

The local refraction index error Δn was included as a state in the covariance analysis. At aircraft approach initiation, the uncertainty in knowledge of the refraction error state was defined by $\Delta n \sim N(0, 10^{-6}\sigma_N)$. For the nominal error model, we assumed $\sigma_N = 10$ and $h_0 = 7000$ m, but these values were varied in the sensitivity analysis.

Ionospheric Spatial Gradient

The differential ranging error due to ionospheric spatial gradient was also modeled in this analysis using the associated LAAS model [9]:

$$\varepsilon_I(i, k) = VIG_i \cdot x(k) \Big/ \sqrt{1 + \left(\frac{R_e \cos E(i, k)}{R_e + h_I}\right)^2} \quad (2)$$

where ε_I is the L1 ionospheric error (negative for carrier), VIG is the vertical ionospheric gradient, h_I is the ionospheric shell height (350 km), R_E is the earth's radius, and x is the distance of the airplane from the ship. (E, i and k are as defined earlier.)

In the covariance analysis, an independent VIG state was included for each satellite. At aircraft approach initiation, the uncertainty in knowledge of each VIG state was defined by $VIG_i \sim N(0, \sigma_{VIG})$. For a nominal error model, we assumed $\sigma_{VIG} = 1$ mm/km, but this parameter was also varied in the sensitivity analysis.

Floating-Ambiguity and Fixed-Integer Implementation Models

During each simulated approach, both aircraft and satellite motion were modeled. The state covariance matrix (including floating cycle ambiguity, position, and error model states) was propagated in time during the approach. For *floating-ambiguity implementation* results, only the standard deviation of the time history vertical position error σ_{vert} (a direct output of the covariance propagation) was of interest. The basic performance criterion used in this analysis was the vertical protection level under fault-free (H0) conditions (VPL_{H0}), defined by

$$\text{Prob}\left\{|\hat{x}_{vert} - x_{vert}| > VPL_{H0}\right\} = 10^{-7} \Rightarrow$$
$$VPL_{H0} = 5.33\sigma_{vert} \quad (3)$$

It is important to note that equation (3) implicitly assumes a normal error distribution for vertical error. This is not to say that the vertical error itself or the component error sources must actually be Gaussian, but rather that σ_{vert} must be established such that a Gaussian cumulative error distribution with this value of standard deviation will overbound the actual cumulative error distribution at the probability level of interest. Careful consideration of such error overbounding is currently being pursued for LAAS, and the successful resolution of this issue will provide the foundation for the treatment of non-Gaussian errors in SRGPS. In this analysis, all error variances are meant to correspond to overbounding Gaussian distributions. It is also noted that in this initial work, we allocated the total allowable navigation integrity risk (10^{-7}) entirely to the fault-free case. For navigation availability, it is required that $VPL_{H0} < VAL$, where VAL is the specified vertical alert limit (1.1 m). Overall fault-free service availability (A_{FF}) was defined as:

$$A_{FF} = \text{Prob}\{VPL_{H0} < VAL\} \quad (4)$$

For *fixed-integer implementations*, a correct fix (CF) of the cycle ambiguities, or some subset linear combination of those ambiguities, will improve positioning performance such that $\sigma_{vert|CF} < \sigma_{vert}$. Obviously, for a fixed-integer implementation it is desired that the

probability of incorrect fix (P_{IF}) be small. In mathematical terms, the associated VPL_{H0} is defined by

$$\text{Prob}\left\{|\hat{x}_{vert} - x_{vert}| > VPL_{H0}|CF\right\}\cdot(1 - P_{IF}) + \text{Prob}\left\{|\hat{x}_{vert} - x_{vert}| > VPL_{H0}|IF\right\}\cdot P_{IF} = 10^{-7} \quad (5)$$

Given an incorrect fix, it is assumed that the resulting position error will generally be large, so that

$$\text{Prob}\left\{|\hat{x}_{vert} - x_{vert}| > VPL_{H0}|IF\right\} \approx 1 \quad (6)$$

Substituting equation (6) into equation (5), we obtain

$$\text{Prob}\left\{|\hat{x}_{vert} - x_{vert}| > VPL_{H0}|CF\right\} = \frac{10^{-7} - P_{IF}}{1 - P_{IF}} \quad (7)$$

so that

$$VPL_{H0} = k(P_{IF})\cdot\sigma_{vert|CF} \quad (8)$$

The integrity multiplier (k) in equation (8) is plotted as a function of P_{IF} in Figure 2. For very small P_{IF}, the integrity multiplier approaches 5.33, the value in equation (3). However, as P_{IF} approaches 10^{-7}, the integrity multiplier, and hence VPL_{H0}, grows very large. For this analysis, we imposed a reasonable, intermediate requirement on the "fixed" implementation: $P_{IF} < 10^{-8}$. In this case,

$$VPL_{H0} = 5.35\ \sigma_{vert|CF} \quad (9)$$

The fixed-integer implementation model used in this analysis was Teunissen's "Integer Bootstrapping" algorithm with LAMBDA cycle ambiguity decorrelation [10]. The Integer Bootstrapping implementation is a successive rounding approach for which it is possible to directly compute the probability of correct fix (P_{CF}).

An illustrative result for a hypothetical airplane approach is shown in Figure 3. The approach begins at the specified GPS data broadcast radius (at the far right in the figure). As time passes, the aircraft approaches the ship (distance from touchdown grows smaller), and the combined effect of filtering and satellite motion causes σ_{vert} (floating), and therefore VPL_{H0}, to become smaller. At a certain point during the approach, the probability of correct fix may become larger than the minimum required ($1 - 10^{-8}$). From this point on, a fixed solution is possible.

To consolidate the results from a large number of simulated approaches (associated with different satellite geometries and SRGPS parameter values) in a relatively compact way, VPL_{H0} results are presented as illustrated in the right-hand plot in Figure 4. Here, a single curve is used to define the variation in VPL_{H0} at 100 ft altitude with GPS data broadcast radius (DBR) for a given satellite geometry. The satellite geometry is matched (for all of the approaches used to generate the right-hand curve) at the 100 ft altitude point; thus, as DBR increases, the final geometry is the same, but there exists a longer prior exposure time for satellite motion and filtering. In this way, the results for many satellite geometries (many such curves) can be presented on a single plot.

$$VPL_{H0} = 5.35\,\sigma_{vert|CF}\,.$$

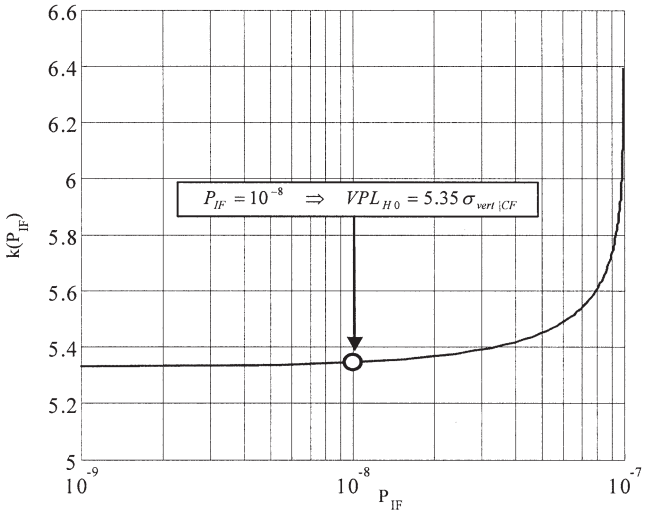

Fig. 2–Integrity Multiplier as a Function of P_{IF}

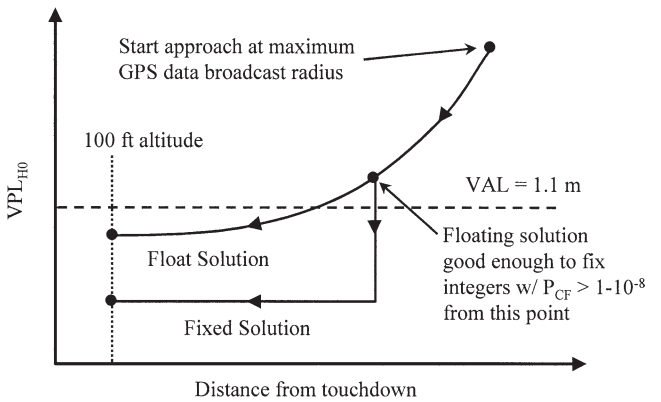

Fig. 3–Evolution of VPL_{H0} for a Single Hypothetical Approach

PERFORMANCE RESULTS

SRGPS fault-free availability was evaluated over an entire day of satellite geometries. The performance of single- and dual-frequency architectures was assessed for both floating-ambiguity and fixed-integer implementations as a function of the standard deviations of code phase (pseudorange) and carrier-phase error, measurement error time constant, and data broadcast radius. In all cases, fixed-integer implementations were constrained to achieve $P_{IF} < 10^{-8}$. Availability results were generated for both the full 24-satellite GPS constellation and depleted GPS constellations. The depleted constellation results were combined to compute overall

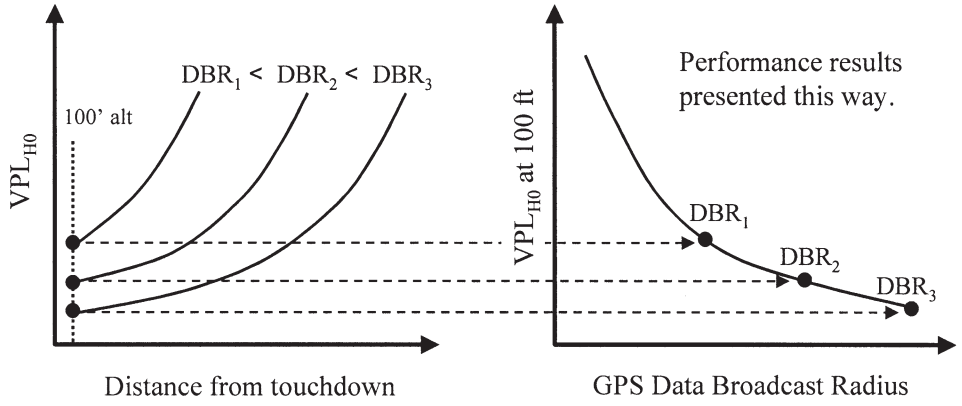

Fig. 4–Format of Plotted Results

average service availability based on the "minimum standard" constellation state probability model given in the GPS Standard Positioning Service Performance Standard [11]. The state probability model is shown in Table 1. The results for the full 24-satellite case, which may be interpreted as upper bounds on availability given the specified error models, were used principally to evaluate the sensitivity of availability results to variations in ionospheric and tropospheric error model parameters and processing architectures (i.e., fixed vs. floating).

A 30-processor parallel PC cluster was used to manage the computational load associated with the processing of aircraft approaches for the large number of satellite outage cases, error model parameter combinations, and broadcast radii. The results presented below quantify the trade-offs between navigation system availability and derived requirements on receiver/antenna performance and data broadcast radius.

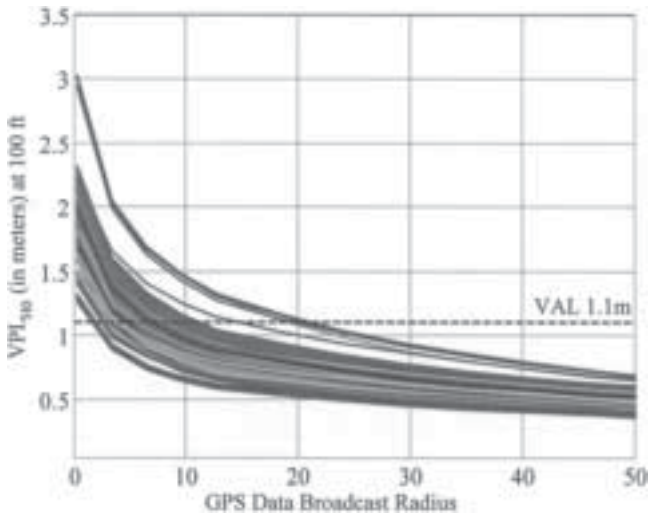

Fig. 5–Full-Day Results, Dual-Frequency Floating-Ambiguity Implementation

Dual-Frequency Performance

Example results for a complete day of satellite geometries are shown in Figures 5 and 6 for floating-ambiguity and fixed-integer implementations, respectively. These results correspond to the full GPS constellation case with specific measurement error values of $\sigma_\phi = 1$ cm, $\sigma_{PR} = 0.3$ m, and $\tau = 40$ s. The nominal ionospheric and tropospheric error models described earlier were also used. By comparing the

Table 1—Satellite Constellation State Probability Model

Number of Healthy Primary Slot Satellites	State Probability
24	0.950
23	0.030
22	0.012
21	0.005
20	0.003

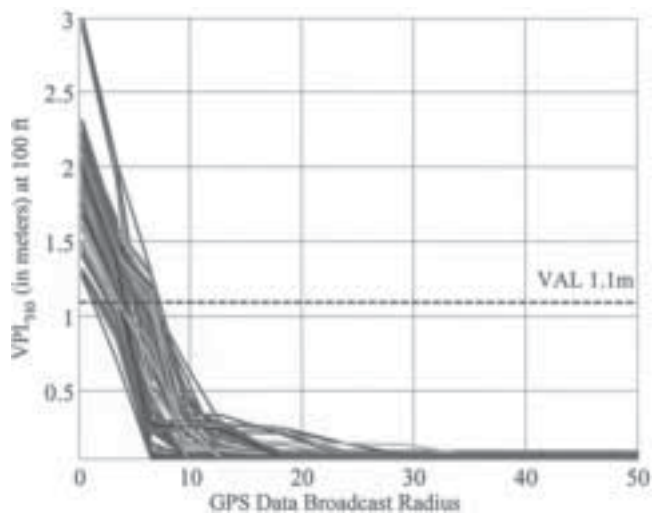

Fig. 6–Full-Day Results, Dual-Frequency Fixed-Integer Implementation

two figures, it is immediately clear that the fixed-integer performance (even with the P_{IF} constraint) is superior to that of the floating-ambiguity implementation in the sense that much smaller DBR values are required to achieve sub-VAL performance.

Figures 7 and 8 show "unavailability" $(1 - A_{FF})$ as a function of DBR using a full constellation for floating-ambiguity and fixed-integer implementations, respectively. These results correspond to error model parameter values of $\sigma_\phi = 1$ cm, $\sigma_{PR} \in \{0.1, 0.15, 0.3\}$ m, and $\tau \in \{40, 60, 120\}$ s. The figures quantify the relative benefits of floating-ambiguity versus fixed-integer implementations directly in terms of availability. Specifically, it is noted that when σ_{PR} is large, the availability provided by the fixed-integer implementation is notably better than that provided by the floating-ambiguity implementation, but when σ_{PR} is small, roughly equivalent availability is achievable using either implementation. This is true because when σ_{PR} is very small (~10 cm), the floating-integer implementation is typically good enough to ensure that VPL_{H0} will be smaller than VAL (1.1 m). Thus any further improvement in accuracy provided by the fixed-integer implementation will not improve availability significantly.

Figure 9 shows analogous (fixed-integer implementation) results to those in Figure 8 for $\sigma_\phi = 1.5$ cm. Comparing Figures 8 and 9, it is evident that availability (or equivalently, required DBR) is much more sensitive to σ_ϕ when σ_{PR} is large. This is true because for small σ_{PR}, code-phase measurements provide a more reliable basis for cycle ambiguity estimation, whereas for large σ_{PR}, cycle resolution performance is more heavily dependent on the quality of redundant carrier-phase measurements.

Common to all three figures is an obvious dependence on measurement error time constant. In general, for a given DBR, the effectiveness of filtering during the approach decreases as the error time constant increases. Conversely, as the error time constant is increased, larger DBRs are required to maintain a constant level of availability. As σ_{PR} is lowered, however, it is true that positioning performance near the ship is less dependent on prior filtering during the approach. In this case, sensitivity to the measurement error time constant is reduced significantly.

Figure 10 shows an interpolated mapping of covariance simulation results using all combinations of error model parameter values derived from the nominal sets defined earlier: $\sigma_{PR} \in \{0.1, 0.15, 0.3\}$ m, $\sigma_\phi \in \{0.5, 1.0, 1.5, 2.0\}$ cm, and $\tau \in \{40, 60, 120\}$ s. This figure specifically relates the receiver error performance characteristics (σ_{PR}, σ_ϕ, τ) and DBR required to provide an availability of 99.7 percent using a full GPS

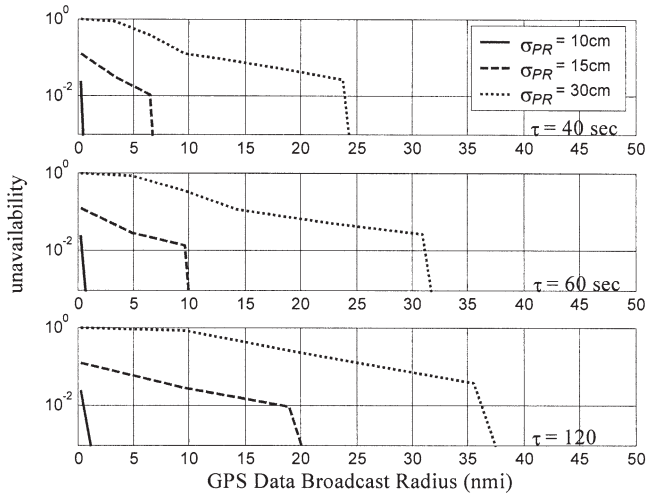

Fig. 7–Availability of Dual-Frequency Floating-Ambiguity Implementation, $\sigma_\phi = 1$ cm (full constellation)

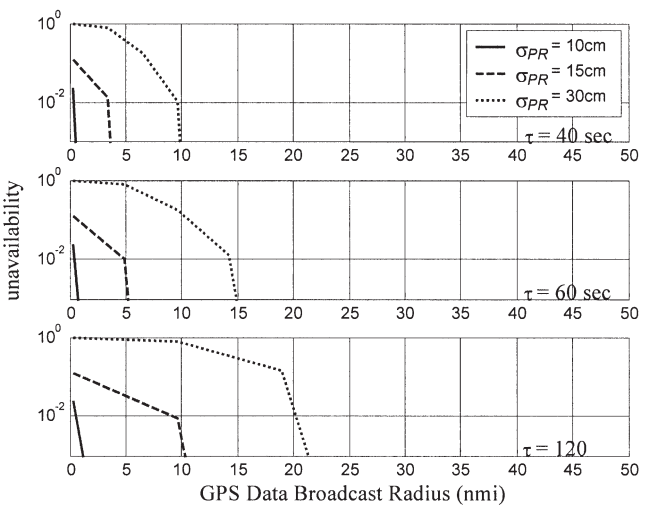

Fig. 8–Availability of Dual-Frequency Fixed-Integer Implementation, $\sigma_\phi = 1$ cm (full constellation)

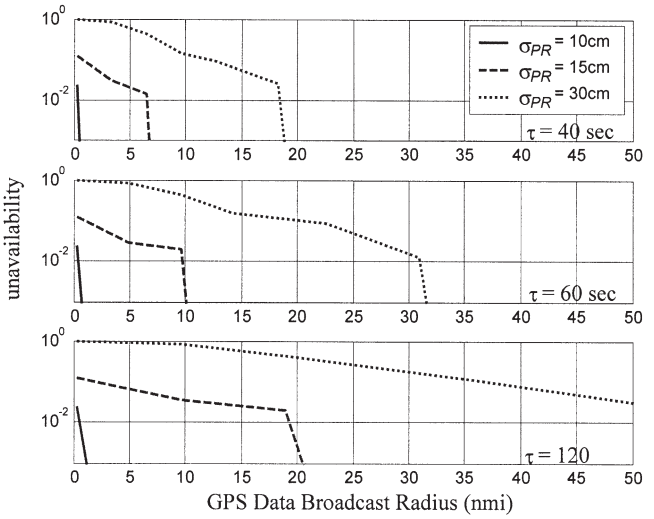

Fig. 9–Availability of Dual-Frequency Fixed-Integer Implementation, $\sigma_\phi = 1.5$ cm (full constellation)

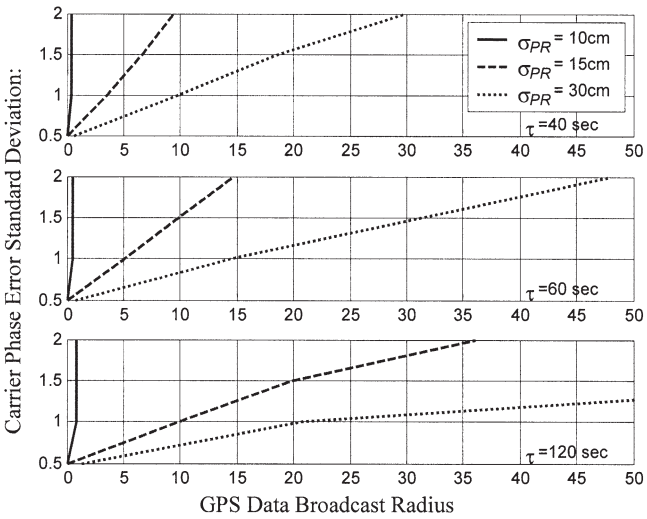

Fig. 10–Dual-Frequency Fixed-Integer Implementation System Requirements to Achieve 0.997 Availability (full constellation)

constellation. For example, for given values of DBR (defined on the horizontal axis), σ_{PR}, and τ (defined by the separate curves), the vertical axes define the necessary values of σ_ϕ to achieve 0.997 availability. The results are encouraging in the sense that 99.7 percent availability is achievable with reasonable receiver error performance characteristics and data broadcast radius (e.g., σ_{PR} = 30 cm, σ_ϕ = 1 cm, τ = 2 min, and DBR = 20 nmi).

When satellite outages were considered, however, more stringent requirements on receiver error performance and DBR were required to achieve 99.7 percent availability. In this regard, Figure 11 shows performance curves using the depleted constellation model in Table 1. As expected, the results are somewhat less favorable than those in Figure 10 (where all satellites were assumed functional). In particular, the poorer satellite geometries cause the system performance to become more sensitive to σ_ϕ, even when σ_{PR} is as small as 10 cm. This result is due simply to the fact even when cycle ambiguities are correctly resolved, the achievable VPL_{H0} is still fundamentally limited by the quality of the satellite geometry and σ_ϕ.

Dual-Frequency Performance Sensitivity

The sensitivity of dual-frequency SRGPS performance results to tropospheric and ionospheric error model parameters was also explored by varying each parameter directly. In addition, the dependency of performance on the effects of satellite motion was examined. The results of these sensitivity analyses for the dual-frequency case are described below.

Satellite Motion

It is well known that satellite motion can be a helpful factor in cycle ambiguity estimation. Over the time scale of an SRGPS aircraft approach, however, it is unclear whether such motion is significant enough to provide measurable benefits beyond those naturally realized from simply filtering code and carrier errors. To investigate the relative benefits of satellite motion for SRGPS, results comparable to those in Figure 8 were regenerated by holding the satellite geometry fixed during the course of each approach. The results of this exercise, shown in Figure 12, reveal little change in the performance relative to Figure 8. In general, the GPS satellite motion is not significant enough over the time scales of interest to affect the performance of a dual-frequency system. The only notable exception occurs for larger values of σ_{PR} and τ. In this case, filtering of code and carrier is less effective, making satellite motion relatively more beneficial.

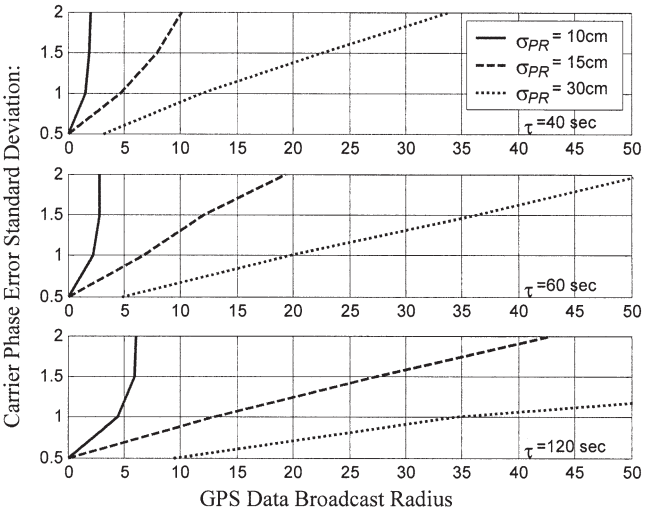

Fig. 11–Dual-Frequency Fixed-Integer Implementation System Requirements to Achieve 0.997 Availability (depleted constellation model)

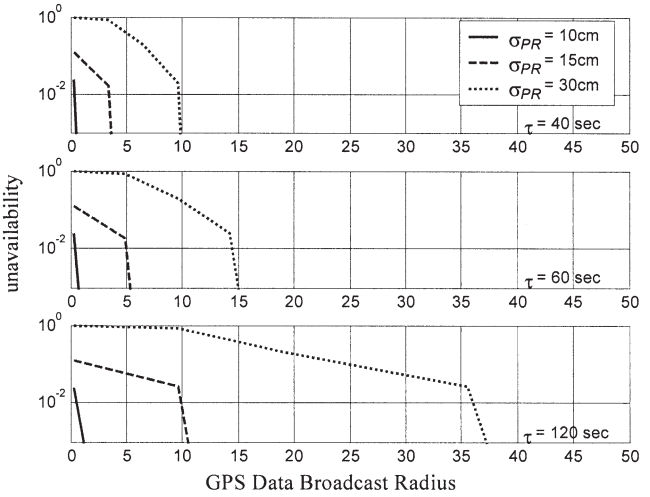

Fig. 12–Dual-Frequency Performance Sensitivity to Satellite Motion, Fixed-Integer Implementation, σ_ϕ = 1 cm (full constellation)

Ionospheric Spatial Gradient

The sensitivity of dual-frequency implementation performance to ionospheric spatial gradient was also investigated. In this regard, Figure 13 shows the availability results when uncertainty in prior knowledge of VIG was increased to $\sigma_{VIG} = 1$ cm/km for each satellite. Because the dual-frequency architecture allows for direct observation of ionosphere gradient during each approach, the performance exhibited here is not significantly different from the nominal case in Figure 8, where $\sigma_{VIG} = 1$ mm/km.

Tropospheric Decorrelation

Figure 14 shows the availability results when the uncertainty in prior knowledge of residual tropospheric refractivity was increased to $\sigma_N = 100$. Compared with the nominal model results ($\sigma_N = 10$) in Figure 8, these results show relatively low sensitivity to uncertainty in residual tropospheric refractivity. The only noteworthy exception occurs when both σ_{PR} and τ are large. In this case, a slightly longer filtering time (larger DBR) is required to achieve the same availability as in the nominal case.

Single-Frequency Performance

The full-day system performance results for a single-frequency SRGPS implementation (using the full GPS constellation and the nominal error models with $\sigma_\phi = 1$ cm and 1.5 cm, respectively) are shown in Figures 15 and 16. It is not surprising that the

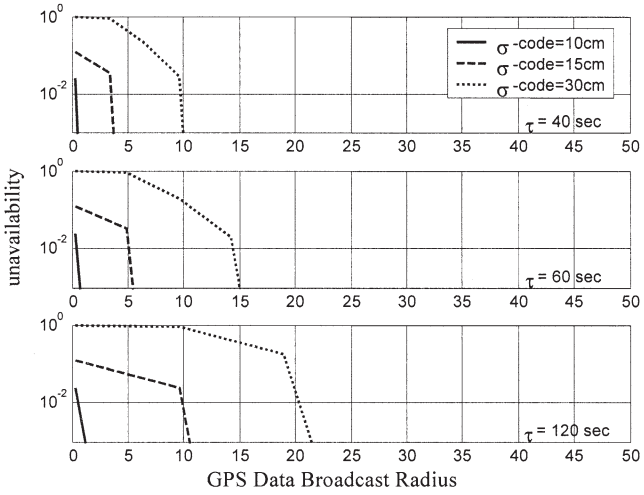

Fig. 13–Dual-Frequency Performance Sensitivity to Ionospheric Gradient Uncertainty, Fixed-Integer Implementation, $\sigma_\phi = 1$ cm (full constellation)

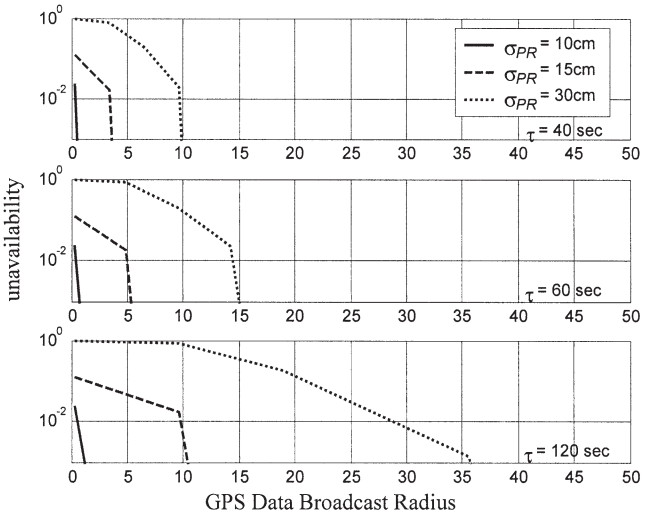

Fig. 14–Dual-Frequency Performance Sensitivity to Residual Tropospheric Decorrelation, Fixed-Integer Implementation, $\sigma_\phi = 1$ cm (full constellation)

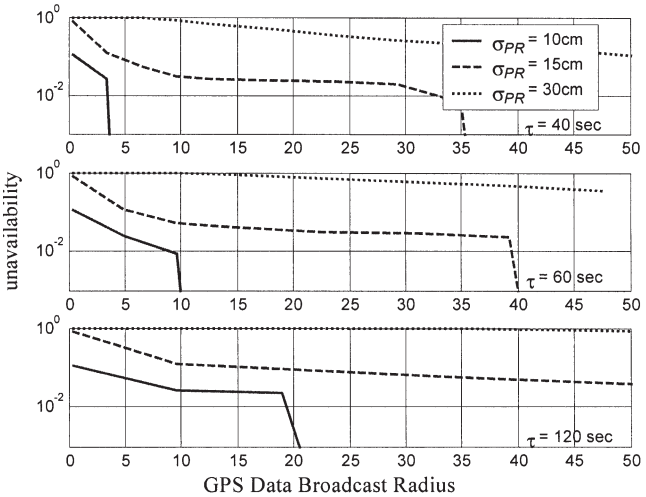

Fig. 15–Availability of Single-Frequency Implementations, $\sigma_\phi = 1$ cm (full constellation)

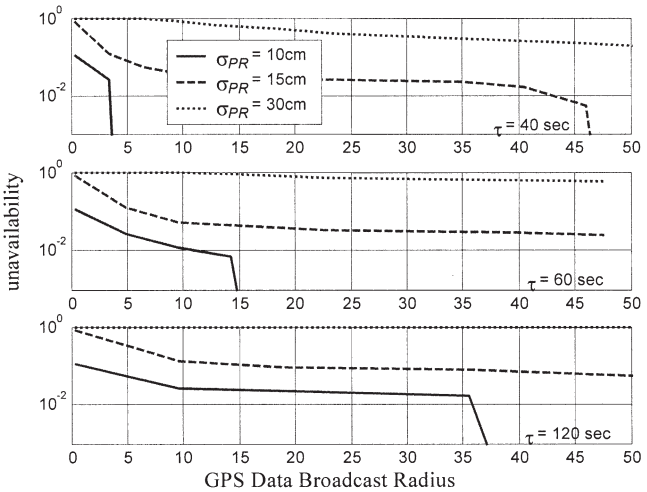

Fig. 16–Availability of Single-Frequency Implementations, $\sigma_\phi = 1.5$ cm (full constellation)

performance here is significantly worse than that for the dual-frequency case (see for comparison Figures 8 and 9). In these results, differentiation between the floating-ambiguity and fixed-integer single-frequency implementations is unnecessary since the availability results for both cases are the same. This is true because whenever integer fixing is possible under the integrity constraint $P_{IF} < 10^{-8}$, the value of VPL_{H0} for the floating-ambiguity implementation is typically already below VAL. Therefore, while integer fixing can improve accuracy, it does not affect availability.

Figure 17 quantifies the receiver error performance characteristics (σ_{PR}, σ_{ϕ}, τ) and DBR required to provide an availability of 99.7 percent given a full GPS constellation. Compared with the dual-frequency system requirements seen earlier in Figure 10, the single-frequency results reveal that 99.7 percent availability is achievable only with significantly more stringent requirements on receiver measurement error performance and larger DBR. Furthermore, as seen in Figure 18, achieving 99.7 percent availability is even more difficult when satellite outages are considered. The stringent system requirements defined in the figure suggest that 99.7 percent availability is likely an unrealistic goal for a single-frequency SRGPS architecture. Nevertheless, the lower availability obtained using single-frequency processing may be sufficient to provide backup capability for a nominal dual-frequency architecture in the event of interference or jamming at one of the two GPS frequencies. For example, Figure 19 shows that the single-frequency system requirements to provide 95 percent availability are much less stringent.

Single-Frequency Performance Sensitivity

For completeness, the sensitivity analyses performed for the dual-frequency case were repeated for the single-frequency architecture. The results are described briefly here.

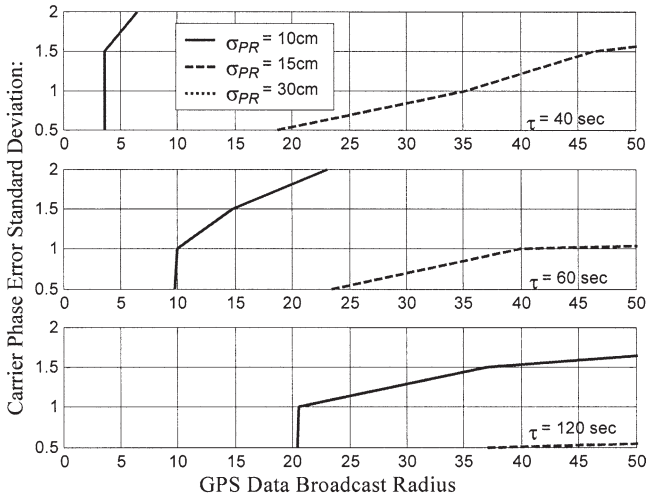

Fig. 17–Single-Frequency System Requirements to Achieve 0.997 Availability (full constellation)

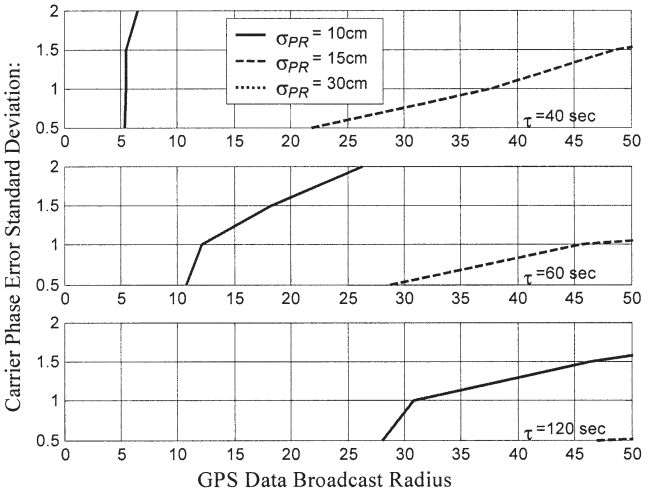

Fig. 18–Single-Frequency System Requirements to Achieve 0.997 Availability (depleted constellation model)

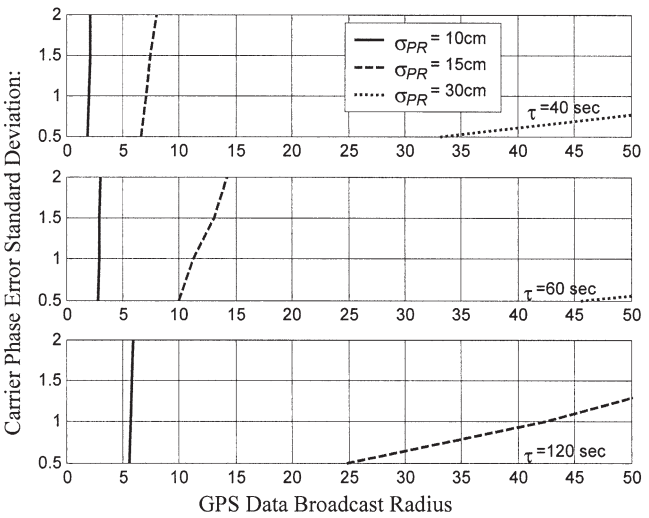

Fig. 19–Single-Frequency System Requirements to Achieve 0.95 Availability (depleted constellation model)

Satellite Motion

As with the dual-frequency case, the relative benefit of satellite motion for a single-frequency SRGPS architecture was evaluated by holding the satellite geometry fixed during the course of each approach. The results are shown in Figure 20. When these results are compared with those in Figure 15 (where the effects of satellite motion were utilized), it is evident that performance is notably worse for the single-frequency case when satellite motion is not exploited. While it is true that the geometry change over the time scale of a typical aircraft is no larger than that

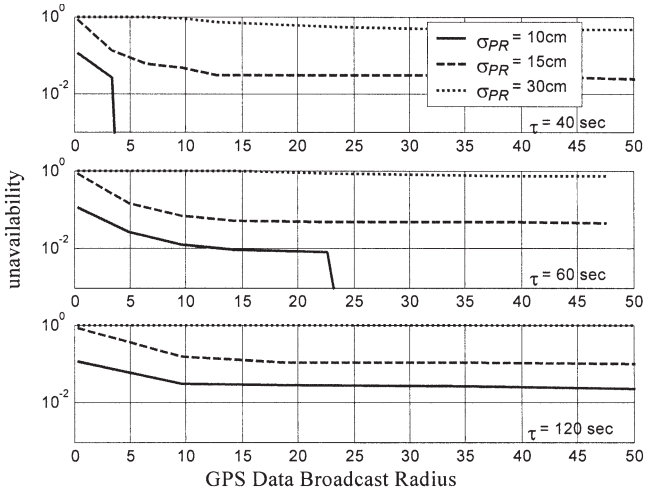

Fig. 20–Single-Frequency Performance Sensitivity to Satellite Motion, σ_ϕ = 1 cm (full constellation)

for the dual-frequency case, its relative importance to cycle ambiguity observability is clearly greater for the single-frequency implementation.

Ionospheric Spatial Gradient

In a general sense, it is expected that a single-frequency implementation will be more susceptible to ionospheric effects than a dual-frequency implementation. This expectation is supported quantitatively in Figure 21, which shows single-frequency implementation availability when the assumed prior knowledge of vertical ionospheric gradient was increased to σ_{VIG} = 1 cm/km for each satellite. In comparison with the single-frequency results in Figure 15 for σ_{VIG} = 1 mm/km, Figure 21 shows significantly greater relative sensitivity to ionospheric spatial gradient than in the dual-frequency case covered earlier.

Residual Tropospheric Decorrelation

Figure 22 shows the availability results when the uncertainty in prior knowledge of residual tropospheric refractivity was increased to σ_N = 100. When these results are compared with those in Figure 15 (where σ_N = 10), it is evident that the availability is only mildly sensitive to uncertainty in residual tropospheric refractivity. Recall that this was also true for the dual-frequency case.

PREFILTERING

In this analysis, it was assumed that filtering of ranging measurements was initiated at broadcast radius entry. In practice, of course, it is possible to begin code-carrier smoothing earlier. For dual-frequency systems, the effect of prior measurement smoothing can be especially important because long filter time constants can be used. One particularly significant implication is that a smaller data broadcast radius may be sufficient to provide the desired level of availability. In addition to the obvious desirability of a small data broadcast radius from a data link design perspective, it is also important to note that an SRGPS solution that relies on a relatively small data broadcast radius will be implicitly more robust to spatial decorrelation (tropospheric and ionospheric) error model assumptions. In contrast, for single-frequency implementations, prefilter time constants must be limited to ensure that any transient filter response to ionospheric divergence will have settled when differential processing begins. As a result, the benefits provided by prefiltering will be much less significant for

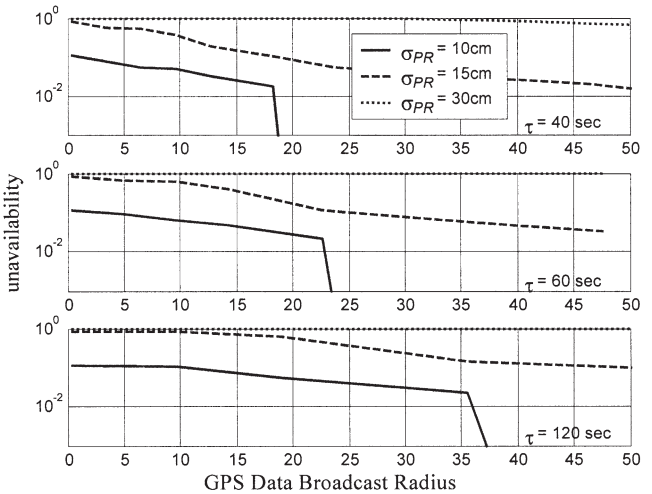

Fig. 21–Single-Frequency Performance Sensitivity to Ionospheric Gradient Uncertainty, σ_ϕ = 1 cm (full constellation)

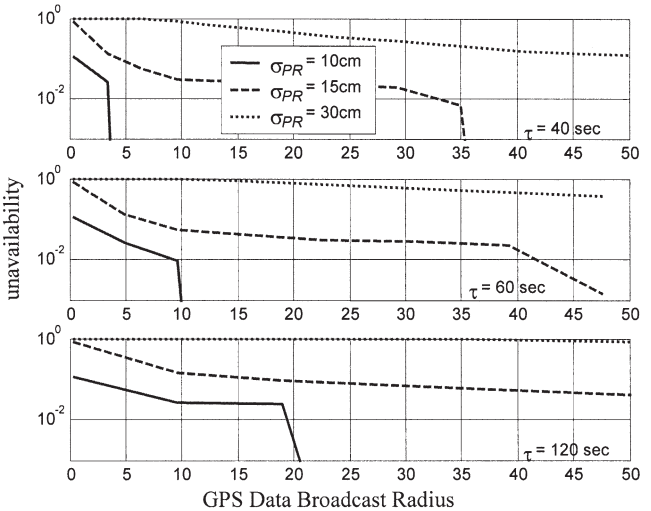

Fig. 22–Single-Frequency Performance Sensitivity to Residual Tropospheric Decorrelation, σ_ϕ = 1 cm (full constellation)

a single-frequency architecture. The effects of prefiltering for both the single- and dual-frequency cases are presently being quantified, and the results will be disseminated in a future paper.

SUMMARY

In this paper, fault-free SRGPS performance has been quantified as a function of data broadcast radius and relevant ranging error parameters, including standard deviations and time constants of raw code and carrier measurement errors, ionospheric spatial gradient uncertainty, and residual tropospheric decorrelation uncertainty. The results demonstrate that for dual-frequency architectures, a fixed-integer realization is superior to a floating-ambiguity implementation, even when stringent constraints on the probability of correct integer resolution are applied. Moreover, the receiver measurement error performance and data broadcast radius required to achieve a system availability of 99.7 percent have been parametrically quantified for both full and depleted GPS satellite constellations. It has also been shown that for a single-frequency architecture, no availability benefit is derived from the use of a fixed-integer implementation (relative to floating-ambiguity processing). Although achieving 99.7 percent availability is likely an unrealistic goal for a single-frequency architecture, in the event of interference or jamming at one of the two GPS frequencies, single-frequency processing could provide sufficient availability to function as a backup for a nominal dual-frequency/fixed-integer architecture.

ACKNOWLEDGMENTS

The constructive comments and advice regarding this work provided by Frank Allen, John Clark, Ian Gallimore, Dennis King, Marie Lage, and Ken Wallace are greatly appreciated. The authors gratefully acknowledge the U.S. Navy (Naval Air Warfare Center) for supporting this research. However, the views expressed in this paper belong to the authors alone and do not necessarily represent the position of any other organization or person.

Based on a paper presented at The Institute of Navigation's ION GPS-2001, Salt Lake City, Utah, September 2001.

REFERENCES

1. JPALS Test Planning Working Group, *Architecture and Requirements Definition: Test and Evaluation Master Plan for JPALS*, January 19, 1999.
2. *Operational Requirements Document (ORD) for Joint Precision Approach and Landing System (JPALS)*, USAF 002–94-I.
3. Waters, J., P. Sousa, L. Wellons, G. Colby, and J. Weir, *Test Results of an F/A-18 Automatic Carrier Landing Using Shipboard Relative GPS*, Proceedings of The Institute of Navigation's Annual Meeting, Albuquerque, NM, June 11–13, 2001.
4. Brown, A. and N. Gerein, *Test Results from a Digital P(Y) Code Beamsteering Receiver for Multipath Minimization*, Proceedings of The Institute of Navigation's Annual Meeting, Albuquerque, NM, June 11–13, 2001.
5. Koenig, M., D. Gebre-Egziabher, S. Pullen, U. S. Kim, B. Pervan, and F. C. Chan, *Analysis of Reference Antenna Motion on the JPALS Shipboard Integrity Monitor*, Proceedings of The Institute of Navigation's National Technical Meeting, Anaheim, CA, January 2002.
6. Colby, G., *JPALS Navy Program and Requirements Overview*, Briefing to SRGPS Architecture Integrated Product Team, March 6, 2001.
7. Wallace, K., Personal Communication, August 13, 2001.
8. RTCA SC-159, *Minimum Operational Performance Standards for Global Positioning System/Wide Area Augmentation System Airborne Equipment* (RTCA/DO-229C), Washington, D.C., October 6, 1999.
9. McGraw, G., T. Murphy, M. Brenner, S. Pullen, and A. J. Van Dierendonck, *Development of the LAAS Accuracy Models*, Proceedings of The Institute of Navigation's ION GPS-2000, Salt Lake City, UT, September 19–22, 2000.
10. Teunissen, P., D. Odijk, and P. Joosten, *A Probabilistic Evaluation of Correct GPS Ambiguity Resolution*, Proceedings of The Institute of Navigation's ION GPS-98, Nashville, TN, September 15–18, 1998.
11. Department of Defense, *Global Positioning System Standard Positioning Service Performance Standard*, October 2001.